Supplemental Material

to

Expression of Fusion Proteins of *Aspergillus terreus* Reveals a Novel Allene Oxide Synthase

by

Inga Hoffmann, Fredrik Jernerén, and Ernst H. Oliw

From the Division of Biochemical Pharmacology, Department of Pharmaceutical Biosciences, Uppsala Biomedical Center, Uppsala University, SE-75124, Uppsala, Sweden

1. FIGURE LEGENDS

Fig. S1. LC-MS/MS analysis of the apparent D-KIE of 9*R*-DOX. The first and second chromatograms show the signal intensities of the internal standard (13-HOTrE) and 9*R*-HODE, respectively. The latter was obtained after incubation with [$^{13}C_{18}$]18:2n-6 and reduction to the alcohol. The third and fourth chromatograms show the signal intensities of the internal standard and 9*R*-HODE obtained after oxygenation of [11,11-2H2]18:2n-6, respectively and reduction to the alcohol. The signal intensities suggest a D-KIE of ~4.1.

Fig. S2. Western blot analysis of recombinant ATEG. A, ATEG_04755, 03171, and 03992 were obtained from expression in insect cells (*Sf21*), ATEG_02036 from expression in insect cells (*Sf*9), and ATEG_03992_sv, 00985, and 03580 from expression in *E. coli* (BL21). B, Western blot analysis of AOS·C1073S, AOS·N964D, and AOS·N964V, all obtained from expression in *E. coli* (BL21). The position of the protein size ladder was approximately as indicated.

Fig. S3. HPLC-MS/MS analysis of alcohols obtained from recombinant ATEG_03171, 04755, and 00985 after incubations with 18:2n-6 and reduction. Left, Analysis of 10-HODE obtained from incubation of recombinant ATEG_03171 and 18:2n-6. The top and bottom chromatograms show chiral separation of the characteristic ions (MS^2 *m/z* 295 → 183 and 155, respectively, demonstrating that the *R*-stereoisomer is mostly formed). Middle, RP-HPLC-MS/MS analysis of 10-HODE formed by ATEG_04755. Right, Chiral separation of 8-HODE (MS^2 *m/z* 295 → 157) formed from 18:2n-6 by recombinant ATEG_00985 indicating that the *R*-stereoisomer predominated.

Fig. S4. LC-MS analysis of trapped allene oxide. A, NP-HPLC-MS/MS analysis of 9-hydroxy-10-methoxy-octadecadecenoic acid obtained after short time incubation of AOS with 9*R*-HPODE, yielding 9(10)-EODE, which was trapped with methanol. B, MS/MS spectrum of 9-hydroxy-10-methoxy-octadecadecenoic acid (MS^2 *m/z* 325 → full scan) with characteristic ions, *m/z* 307 (A^- -18), 293 (A^- -32, loss of methanol), and 275 (293-18).

Fig. S5. Fatty acid composition of *A. terreus* grown in liquid medium (2% malt extract). The MS spectrum shows the total scan of fatty acid carboxylate anions from nitrogen powder of mycelia after alkali treatment and extractive isolation analyzed by direct injection.

Fig. S6. Alignment of AOS (ATEG_02036) with 5,8-LDS (ATEG_03992) by ClustalW. This alignment shifts the relative positions of the Thr-Xxx-Xxx-Gly-Xxx-Val-Ala-Asn-Xxx-Xxx-Gln sequences (Fig. 5) six positions (see VANxxQ in line AOS 896 and in line 5,8-LDS 876).

Fig. S7. NP-HPLC-MS/MS analysis of oxidation products of AOS·N964D and AOS·Q967L. The top and bottom chromatograms show the TICs of MS^2 analyses (*m/z* 311→ full scan) obtained after incubations of 9*R*-HPODE with AOS·N964D and AOS·Q967L, respectively.

Fig. S8. Oxidation of 18:2n-6 by 5,8-LDS·Q881K. NP-HPLC-MS/MS analysis of metabolites. TIC of MS^2 311 shows increased relative formation of 7,8- and 8,11-DiHODE metabolites, and *erythro* and *threo* epoxyalcohols in comparison to the native recombinant enzyme.

2. FIGURES

Fig. S1

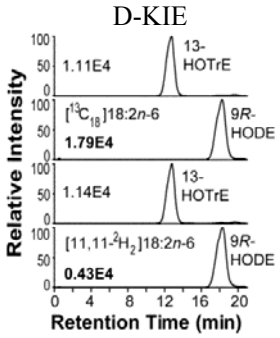

Fig. S2

A

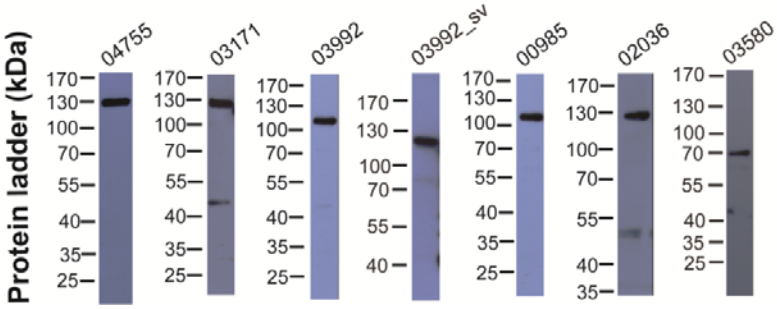

B

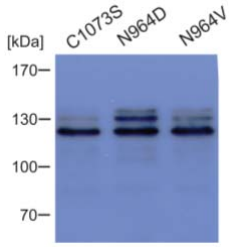

Fig. S3

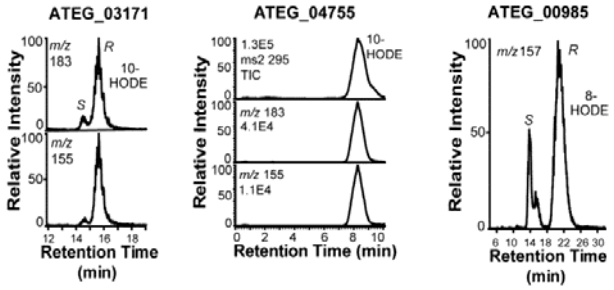

Fig. S4

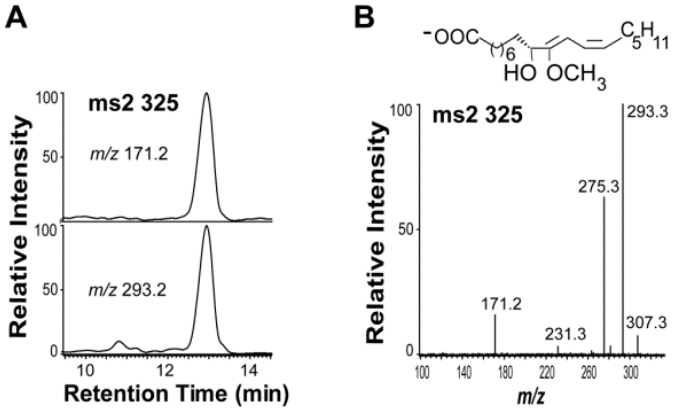

Fig. S5

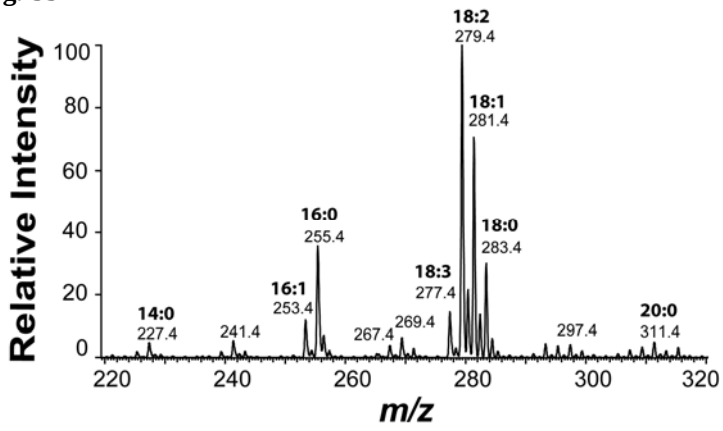

Fig. S6

```
AOS          1 SITGTGVGIWSRLYARIFHSDELAEEEDDEKYQAGEAYGDPKVLATSLIKDLRALGVKGR
5,8-LDS      1 -MQGIGKAISQLEKVATASLRPLPTETGDGSYVA-------ESTATGLVQDLPHVDLG--

AOS         61 RSDLRTLIEMVK--NKGKPMDDRQMHMEKIIAIVAMLPRTSKARQRLTGVLIDQLWRSLQ
5,8-LDS     51 --DLKTLLDVTKNAATGEPIDDKGYVMERLIQLASGLPSTSRNAKQLTSAFLNQLWNDLD

AOS        119 HPPLSYFGNKYQYRTPDGSYNNPLEPNLGKAGSPYARSIPRIKTMHGVRPDPGLLFDLLM
5,8-LDS    109 HPPVSTVGGEYSHRSADGSGNNILWPGIGAAGSHYARSVQPKTMQSPSLPDPEALFDSLL

AOS        179 ARDDSTFKENPAGISSMLFYHASIIIHDIFRTNRRDPNISDTSSYLDLAPLYGSSLEDQL
5,8-LDS    169 ARKD--FKEHPNKISSVLFYIASIIIHDLFQTDHRDSSINRTSSYLDLSPLYGNNQDEQY

AOS        239 KVRTMEKGMLKPDTFHEKRLLGQPAGVNVILVMYSRFHNYVADMLLKINENGRFTLPPTS
5,8-LDS    227 LMRTFKDGKLKPDCFSSKRILGFPPGVGVLLIMFNRFHNYVVEQLAAVNEGGRFTKP---
```

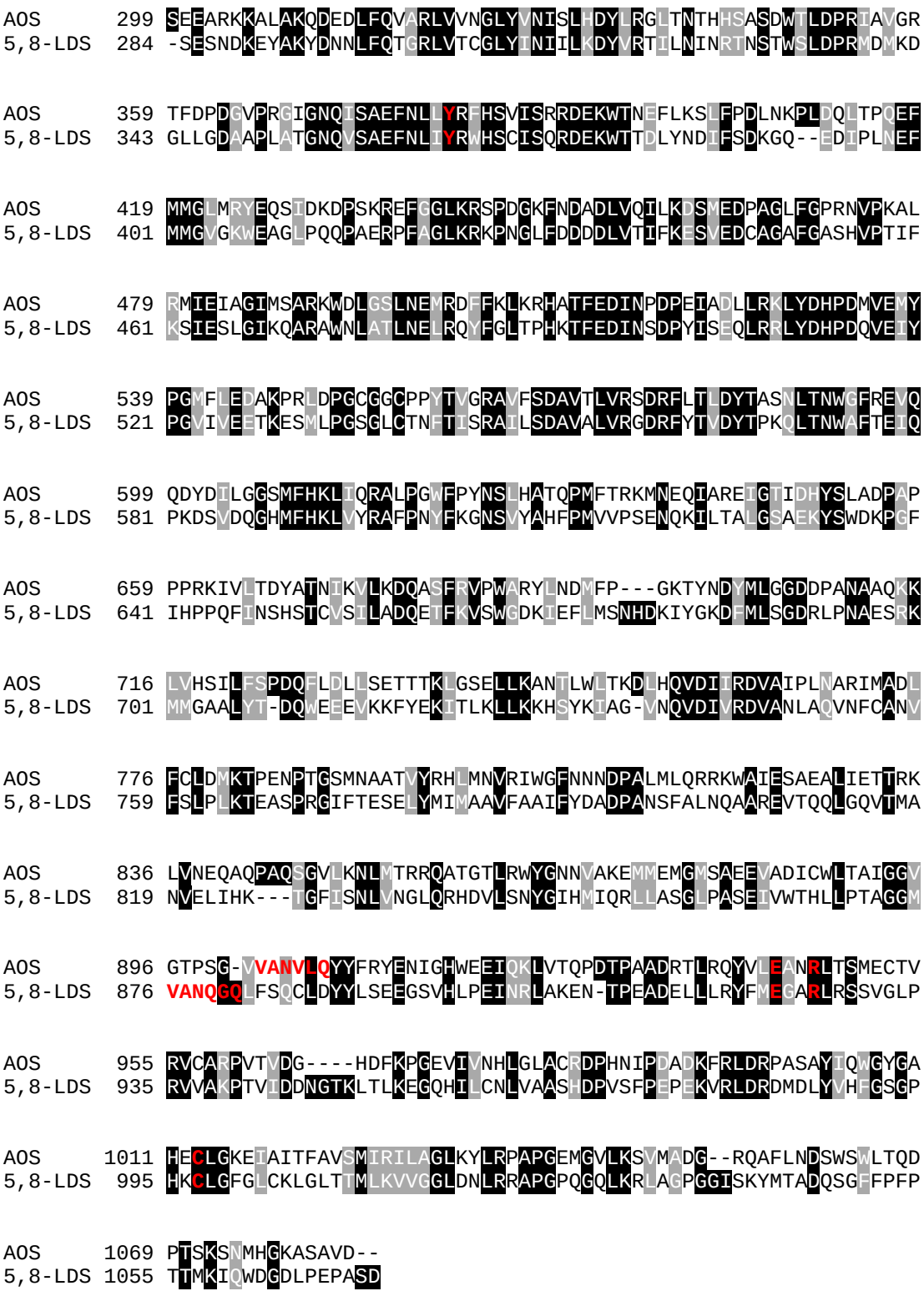
AOS 299 SEEARKKALAKQDEDLFQVARLVVNGLYVNISLHDYLRGLTNTHHSASDWTLDPRIAVGR
5,8-LDS 284 -SESNDKEYAKYDNNLFQTGRLVTCGLYINIILKDYVRTILNINRTNSTWSLDPRMDMKD
AOS 359 TFDPDGVPRGIGNQISAEFNLLYRFHSVISRRDEKWTNEFLKSLFPDLNKPLDQLTPQEF
5,8-LDS 343 GLLGDAAPLATGNQVSAEFNLIYRWHSCISQRDEKWTTDLYNDIFSDKGQ--EDIPLNEF
AOS 419 MMGLMRYEQSIDKDPSKREFGGLKRSPDGKFNDADLVQILKDSMEDPAGLFGPRNVPKAL
5,8-LDS 401 MMGVGKWEAGLPQQPAERPFAGLKRKPNGLFDDDDLVTIFKESVEDCAGAFGASHVPTIF
AOS 479 RMIEIAGIMSARKWDLGSLNEMRDFFKLKRHATFEDINPDPEIADLLRKLYDHPDMVEMY
5,8-LDS 461 KSIESLGIKQARAWNLATLNELRQYFGLTPHKTFEDINSDPYISEQLRRLYDHPDQVEIY
AOS 539 PGMFLEDAKPRIDPGCGGCPPYTVGRAVFSDAVTLVRSDRFLTLDYTASNLTNWGFREVQ
5,8-LDS 521 PGVIVEETKESMLPGSGLCTNFTISRAILSDAVALVRGDRFYTVDYTPKQLTNWAFTEIQ
AOS 599 QDYDILGGSMFHKLIQRALPGWFPYNSLHATQPMFTRKMNEQIARETGTIDHYSLADPAP
5,8-LDS 581 PKDSVDQGHMFHKLVYRAFPNYFKGNSVYAHFPMVVPSENQKILTALGSAEKYSWDKPGF
AOS 659 PPRKIVLTDYATNIKVLKDQASFRVPWARYLNDMFP---GKTYNDYMLGGDDPANAAQKK
5,8-LDS 641 IHPPQFINSHSTCVSILADQETFKVSWGDKIEFLMSNHDKIYGKDFMLSGDRLPNAESRK
AOS 716 LVHSILFSPDQFLDLLSETTTKLGSELLKANTLWLTKDLHQVDIIRDVAIPLNARIMADL
5,8-LDS 701 MMGAALYT-DQWEEEVKKFYEKITLKLLKKHSYKIAG-VNQVDIVRDVANLAQVNFCANV
AOS 776 FCLDMKTPENPTGSMNAATVYRHLMNVRIWGFNNNDPALMLQRRKWAIESAEALIETTRK
5,8-LDS 759 FSLPLKTEASPRGIFTESELYMIMAAVFAAIFYDADPANSFALNQAAREVTQQLGQVTMA
AOS 836 LVNEQAQPAQSGVLKNLMTRRQATGTLRWYGNNVAKEMMEMGMSAEEVADICWLTAIGGV
5,8-LDS 819 NVELIHK---TGFISNLVNGLQRHDVLSNYGIHMIQRLLASGLPASEIVWTHLLPTAGGM
AOS 896 GTPSG-VVANVLQYYFRYENIGHWEEIQKLVTQPDTPAADRTLRQYVLEANRLTSMECTV
5,8-LDS 876 VANQGQLFSQCLDYYLSEEGSVHLPEINRLAKEN-TPEADELLLRYFMECARLRSSVGLP
AOS 955 RVCARPVTVDG----HDFKPGEVIVNHLGLACRDPHNIPDADKFRLDRPASAYIQWGYGA
5,8-LDS 935 RVVAKPTVIDDNGTKLTLKEGQHILCNLVAASHDPVSFPEPEKVRLDRDMDLYVHFGSGP
AOS 1011 HECLGKEIAITFAVSMIRILAGLKYLRPAPGEMGVLKSYMADG--RQAFLNDSWSWLTQD
5,8-LDS 995 HKCLGFGLCKLGLTTMLKVVGGLDNLRRAPGPQGQLKRLAGPGGISKYMTADQSGFFPFP
AOS 1069 PTSKSNMHGKASAVD--
5,8-LDS 1055 TTMKIQWDGDLPEPASD

Fig. S7

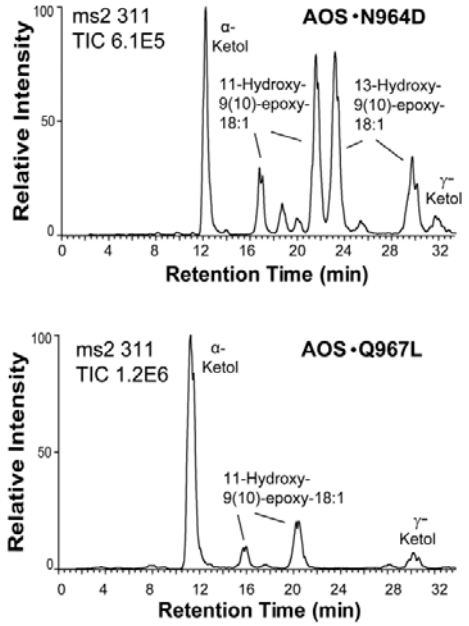

Fig. S8

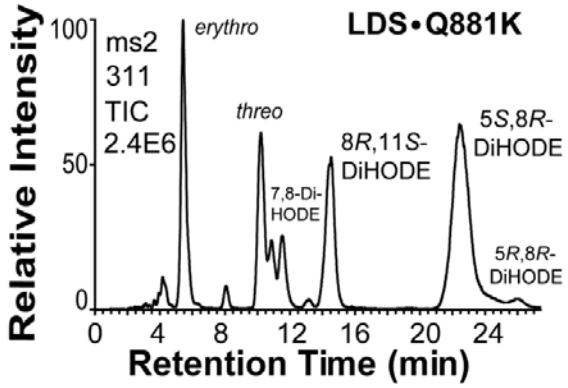

3. METHODS - CLONING AND EXPRESSION IN INSECT CELLS

ATEG_00985, 02036, 04755, and 03580 – All genes were amplified in two pieces from cDNA by PCR or semi-nested PCR technology. Primers F1 and R1 yielded the 5'-fragments and primers F2 and R2 the 3' fragments, respectively. F1 and R2 primers introduced unique restriction sites needed for further cloning steps, and R2 primers also disrupted the native stop codons. Fragments were cloned into pJET1.2/blunt and all genes were assembled by using unique restriction sites (00985: AsisI, 02036: XcmI, 04755: SacII, 03580: XbaI) in their overlapping regions. Subcloning to expression vector pIZ/V5-His was performed using SpeI and XbaI (for 03580: KpnI/SacII) so that all constructs were in frame with the V5 and 6xHis-tag.

ATEG_03171 – An 1806-bp 5'-fragment including introns 1-3 was amplified using primer $03171F_1$ and $03171R_1$ from genomic DNA. A smaller fragment of 784-bp was amplified from cDNA using the same forward primer as above, along with primer $03171R_{E1}$. Both amplicons were subcloned into pJET1.2/blunt and were subsequently combined into a 1657-bp 5'-fragment of cDNA lacking intron 1-3 using SpeI/EcoRI. A 1796-bp 3'-fragment was amplified from cDNA using primer $03171F_2$ and $03171R_2$ and ligated into pJET1.2. The reverse primer disrupted the stop codon and

introduced a downstream XbaI site. Full-length cDNA was generated using EcoRI and XbaI in pJET1.2, and ligated into pIZ/V5-His using SpeI/XbaI in-frame with the V5 epitope and 6xHis-tag, yielding pIZ/V5-His_03171.

ATEG_03992 – ATEG_03992 was cloned from cDNA in two pieces. The 1738-bp 5'-fragment was generated by PCR with primers 03992F1 and 03992R1. 03992F1 introduced a SpeI site. PCR with F2 and R2 yielded in addition to the expected amplicon of 1607-bp an amplicon of 1672-bp. The latter was a splice variant of fragment two and is designated fragment 2sv. Primer R2 disrupted the stop codon and introduced EcoRV sites. All three amplicons were cloned into pJET1.2/blunt. Fragment 1 was combined with fragment 2 and fragment 2sv, respectively, by PCR technology. Subcloning of ATEG_03992 and ATEG_03992sv to expression vector pIZ/V5-His was performed using SpeI and EcoRV restriction sites.

4. RESULTS - CLONING AND EXPRESSION

ATEG_03171 (10R-DOX activity) – The deduced amino acid sequence of ATEG_03171 (GenBank, AFB71132) of the strain IBT1948 differed from the deduced protein (EAU36445) at 17 positions (K63E, H67R, L194W, S205T, K291R, P349R, M702T, V708I, T758I, S761G, D850N, G983A, N987H, K1016N, I1017V, V1072A, M1091K, and M1110T).
ATEG_03171 converted 18:2n-6 to small amounts of 10-HODE, and CP-HPLC-MS/MS analysis revealed that the *R* stereoisomer dominated (Fig. S4). The enzyme activity was two orders of magnitude lower than obtained with recombinant 10*R*-DOX. It is therefore possible that ATEG_03171 oxidizes other substrates than fatty acids more efficiently.

ATEG_00985 (orphan) – Cloning of ATEG_00985 revealed a cDNA fragment of 3183-bp that differed in several nucleotides from the predicted sequence (GenBank, EAU37742.1). We observed the following amino acid exchanges: M116S, S117N, Q118N, and N184D. The residues TLLARKGPAKEHPTRVSSTLFYLATIIIH and VTCS follow residues D145 and L300, respectively, and derive from different exon-intron borders compared to the predicted sequence. An additional intron including genomic nt 3321-3374 (gta…cag) leads to loss of V845-Q862 in the predicted amino acid sequence.

Sequence alignment showed 5,8-LDS as its closest relatives (Fig 2A). The recombinant protein did not transform 9*R*- or 8*R*-HPODE, but oxidized 18:2n-6 to small amounts of 8-HODE and the *R* stereoisomer dominated (Fig. S4). Since this protein did not have AOS or 9*R*-DOX activities, it was not further investigated.

ATEG_03580 (orphan; DOX domain) – Cloning of ATEG_03580 yielded a cDNA fragment of 1851-bp with four introns as predicted (GenBank, EAU35382.1) and no amino acid substitutions. This protein thus lacked the CYP domain. We could not detect significant oxidation of C_{18} fatty acids by the recombinant protein, and it was not further investigated.

5. TABLES

Table S1. Oligonucleotides used for real-time PCR analysis.

Primer pairs	Sequences
qF-03580-alt	5'-gctccggtgttaaccacttt
qR-03580-alt	5'-aaataccctggtgaaagggc
qF-06973-alt	5'-tgaagctctcttccagccta
qR-06973-alt	5'-tgaccttcatggaagaggga
qF-03992fl-alt	5'-ctggcacggaaagacttcaa
qR-03992fl-alt	5'-ttgctcgagaagcaatctgg
ATEG_04755-F	5'-gaggctcagaccgacttcac
ATEG_04755-R	5'-ccgagaccgaactggatgta
ATEG_00985-F(3)	5'-aactgatcgatctctacctgtcc
ATEG_00985-R(3)	5'-atggtagaatccttcgttacctc
ATEG_03171-F	5'-gtttaacctcgcccgtga

ATEG_03171-R	5’-accctctccgtagtggaggt
ATEG_02036-F	5’-gccaaccgtctgaccagtat
ATEG_02036-R	5’-gtccagccggaatttatcg

Table S2. List of cloning primers.

Primer pairs	Sequences
00985F1	5´-ACTAGTatgacgtacaacgatagaagg
00985R_1	5’-gttagattgaccgggccatag
00985F_2	5’-gtggccatactgtcagatgcag
00985R_2	5’-TCTAGATaaatactatcaaatagtgccttc
02036 F_1	5’-ACTAGTatgtcctctgtcatcgttgc
02036 R_1	5’-caagcgtgacagcatcactg
02036 F_2	5’-agacatggtcgaaatgtatcc
02036 R_2	5’-GTTCTAGAAagtccactgcgcttgc
04755 F_1	5’-ACTAGTatgttgcggaggttttctacc
04755 R_1	5’-ttgtagtcgatcgtgtaatgacg
04755 F_2	5’-ctgttctatcggatgcagtggc
04755 R_2	5’-TCTAGATacgcggaggcgattccgcgct
03580 F_1	5’-GGTACCatggagccacccaatttc
03580 R_1	5’-tggattcccagcgttatcacg
03580 F_2	5’-gcgcaccaaacacaaggatg
03580 R_2	5’-CCGCGGtcccttgtatgctgcagac
03171 F_1	5’-ActAGTatgaaattcaaccagaccacag
03171 R_1	5’-gcttcaatttgaagaacttgcg
03171 R_{E1}	5’-ggtggccggtttggaagatat
03171 F_2	5’-atagagcaggcacgcaagtg
03171 R_2	5’-TCTAGAtaaaccggtccatcgaaatg
03992 F_1	5’-ACTAGTatgcagggaattggaaaagc
03992 R_1	5’-ccgtgaaagcccaattggtaag
03992 F_2	5’-tctgcaccaacttcacaatctcg
03992 R_2	5’-GATATCatccgaggcaggttcaggc

Table S3. Oligonucleotides used for subcloning into pET101D-TOPO

Primer pairs	Sequences
Cham04755F	5’-CACCatgttgcggaggttttctac
Cham04755R	5’-cgcggaggcgattccgcgcttcttc
Cham03580F	5’-CACCatggagccacccaatttcc
Cham03580R	5’-tcccttgtatgctgcagactcagg
Champ_03992fl_F	5’-CACCatgcagggaattggaaaag
Champ_03992fl_R	5’-atccgaggcaggttcaggcaaatc
Cham03992_svR	5’-tgtacttggaaatcccaccaggcc
Champ_00985_F	5’-CACCatgacgtacaacgataga
Champ_00985_R	5’-aatactatcaaatagtgccttctt
Cham_02036_F	5’-CACCatgtcctctgtcatcgttg
Cham_02036_R	5’-gtccactgcgcttgctttgccatg
F-champ_03171	5’-CACCatgaaattcaaccagaccac
R-champ_03171	5’-aaccggtccatcgaaat

Table S4. Oligonucleotides used for site-directed mutagenesis.

Enzyme	5'- Forward primer	5' -Reverse primer
5,8-LDS		
N878L	cggctggcgggatggtagcgCTccaaggacaactcttttcgc	gcgaaaagagttgtccttggAGcgctaccatcccgccagccg
Q879L	ctggcgggatggtagcgaaccTaggacaactcttttcgcaatgc	gcattgcgaaaagagttgtcctAggttcgctaccatcccgccag
Q881L	gatggtagcgaaccaaggacTactcttttcgcaatgccttgac	gtcaaggcattgcgaaaagagtAgtccttggttcgctaccatc
Q881E	gatggtagcgaaccaaggaGaactcttttcgcaatgccttgac	gtcaaggcattgcgaaaagagttCtccttggttcgctaccatc
Q881K	gatggtagcgaaccaaggaAaactcttttcgcaatgccttgac	gtcaaggcattgcgaaaagagttTtccttggttcgctaccatc
Q881D	gatggtagcgaaccaaggaGaCctcttttcgcaatgccttgac	gtcaaggcattgcgaaaagagGtCtccttggttcgctaccatc
Q881N	gatggtagcgaaccaaggaAaCctcttttcgcaatgccttgac	gtcaaggcattgcgaaaagagGtTtccttggttcgctaccatc
AOS		
T957A	cgccattgggggcgttggaGcgccctctggagttgttgccaatg	cattggcaacaactccagagggcgCtccaacgcccccaatggcg
S959A	cattgggggcgttggaacgcccGctggagttgttgccaatgtgc	gcacattggcaacaactccagCgggcgttccaacgcccccaatg
N964V	gccctctggagttgttgccGTtgtgctgcagtactacttccgc	gcggaagtagtactgcagcacaACggcaacaactccagagggc
N964D	gccctctggagttgttgccGatgtgctgcagtactacttccgc	gcggaagtagtactgcagcacatCggcaacaactccagagggc
Q967L	gagttgttgccaatgtgctgTTgtactacttccgctatgaaaac	gttttcatagcggaagtagtacAAcagcacattggcaacaactc